

Structural, Electronic and Optical Properties of ZnO Material Using First Principle Calculation

Jaiveer Singh^{1*}, Vivek Kumar Jain²

Abstract

Structural, electronic and optical properties have been determined by using first principle calculation for ZnO material. In present study, full potential linearized augmented plane wave method has been selected with generalised gradient approximation executed in WIEN2k. Structure of ZnO material stabilises in the Wurtzite form of hexagonal closed packed crystal with lattice constant $a=3.289\text{\AA}$, $c=5.307\text{\AA}$. Density of states and band structure diagram of ZnO material shows semiconductor nature with a energy band gap of 0.65 eV. Reflectivity, dielectric function, optical absorption and conductivity, refractive index, energy loss and extinction coefficient have also been explored as a dependence on photon energy incident on ZnO material.

Keywords: Optical Properties, Electronic Properties, Density of State

INTRODUCTION

The thin film transistor (TFT) in which a dielectric layer is sandwich between two metal gates has been classified as field-effect-transistors (FET). Display devices have become flat and high resolution spectrum of colours in present scenario due to metal oxide semiconductor field effect transistor (MOS-FET) as well as light-emitting diodes (LEDs) in TFTs based electronic devices [1–3]. Thin films based on Zinc oxide (ZnO) are widely used for fabricating such devices due to their exceptional electrical, optical characteristics and excellent uniformity available as display devices [4–15]. One of the most prestigious characteristics of ZnO material has a huge binding energy (60 meV) for excitation. Zinc oxide has a room temperature semiconductor in periodic group II-VI with large direct band gap with ultraviolet optical range at which has been reported as potentially application in Resistive Random Access Memory [4–6], Gas Sensors [7], Diode Laser [8], Solar Cells [9], LEDs [10], Switching Transistors [11] and active-matrix liquid-crystal display (AMLCD) [12]. These devices used sunlight to produce electricity through the transparent LCD panel.

ZnO based composites such as electrode, polycrystalline film, and single crystals have been challenged to the researchers and society due to grain boundaries. Optical transparency, high electron

*Author for Correspondence

Jaiveer Singh
Email: singhjaiveer2006@gmail.com

¹Student, Department of Science, Lal Bahadur Shastri Senior Secondary School, Ranpur Kota, Rajasthan, India

²Associate Professor, Department of Physics, School of Basic and Applied Science, Careers Point University Kota, Rajasthan, India

Received Date: May 05, 2023

Accepted Date: July 06, 2023

Published Date: July 26, 2023

Citation: Jaiveer Singh, Vivek Kumar Jain. Structural, Electronic and Optical Properties of ZnO Material Using First Principle Calculation. Journal of Polymer & Composites. 2023; 11(Special Issue 5): S27–S34.

mobility, stability and flexibility at high temperature are some of the issues related to ZnO thin films [13–15]. ZnO Nano-plates were also synthesized by Gupta et al as sensing device towards ethanol with minimum detection and high response magnitude [16]. Nowadays, density functional theory (DFT) has been acclimated to investigate the various attributions such as electronic band gap and optical properties with existing properties of ZnO material. Harun et al. fabricated nanoparticles of ZnO [17] and compared the electronic results with theoretical studies [18]. Matur et al. proposed ZnO:Mg thin film using first principle calculation [19] and

studied optical properties. Bashyal et al. studied the electronic band gap of ZnO using DFT+U and enhance the value of band gap [20]. Researchers are investigating the doping effect on ZnO based films theoretically as well as experimentally, because doping enhancing conductivity and electronic properties [21–22]. The present study aimed to analyse the structural, electronic and optical properties of ZnO material to explore its potential uses in optoelectronics and photonics devices.

EXPERIMENTAL DETAILS

We have used the WIEN2k package of Code on the basis of full potential linearized augmented plane wave (FP-LAPW) in density function theory with GGA (generalised gradient approximation) [23]. Energy of-7.0 Ry was used to separate the core and valence electronic state with range of order 0.00001 Ry for the convergence and 3000 points for k-mesh Brillouin Zone, were taken for ZnO material. In the present study, we calculated the ground state properties such as structural, optical and electronic properties of ZnO material.

RESULTS AND DISCUSSION

Structure Properties

The unit cell of ZnO material consists of four atoms in hexagonal wurtzite structure. In this structure, Zn positions are taken as $(X=1/3, Y=2/3, Z=0)$; $(X=2/3, Y=1/3, Z=1/2)$; and O positions are $(X=2/3, Y=1/3, Z=7/8)$; $(X=1/3, Y=2/3, Z=3/8)$; with space group P63mc as shown in Figure 1(a) and $2 \times 2 \times 2$ supercell of ZnO material is presented in Figure 1(b).

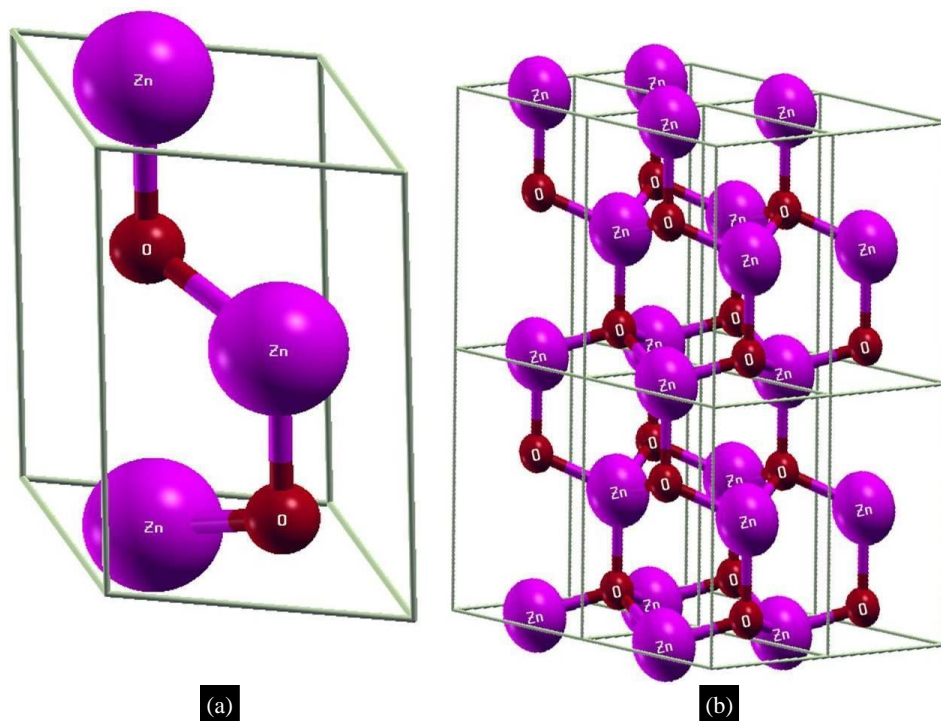


Figure 1. (a) Unit cell of ZnO material and (b) $2 \times 2 \times 2$ supercell of ZnO material.

Volume optimised of ZnO material via energy versus volume curve presented in Figure 2 and find equilibrium lattice constant where energy minimise and also the minimum volume of unit cell at the stable state for further calculations. Optimised lattice constant for ZnO material and compared with previously reported data has been reported (Table 1). It shows that the optimised lattice constant is well matched with the previously obtained lattice constant. The c/a ratio is 1.614 for ZnO material which is well matched with experimentally obtained lattice constant by Harun et al. [18]. The choice of different exchange correlation function gives the different interface boundaries therefore the lattice parameter can be varied accordingly as reported in Table 1.

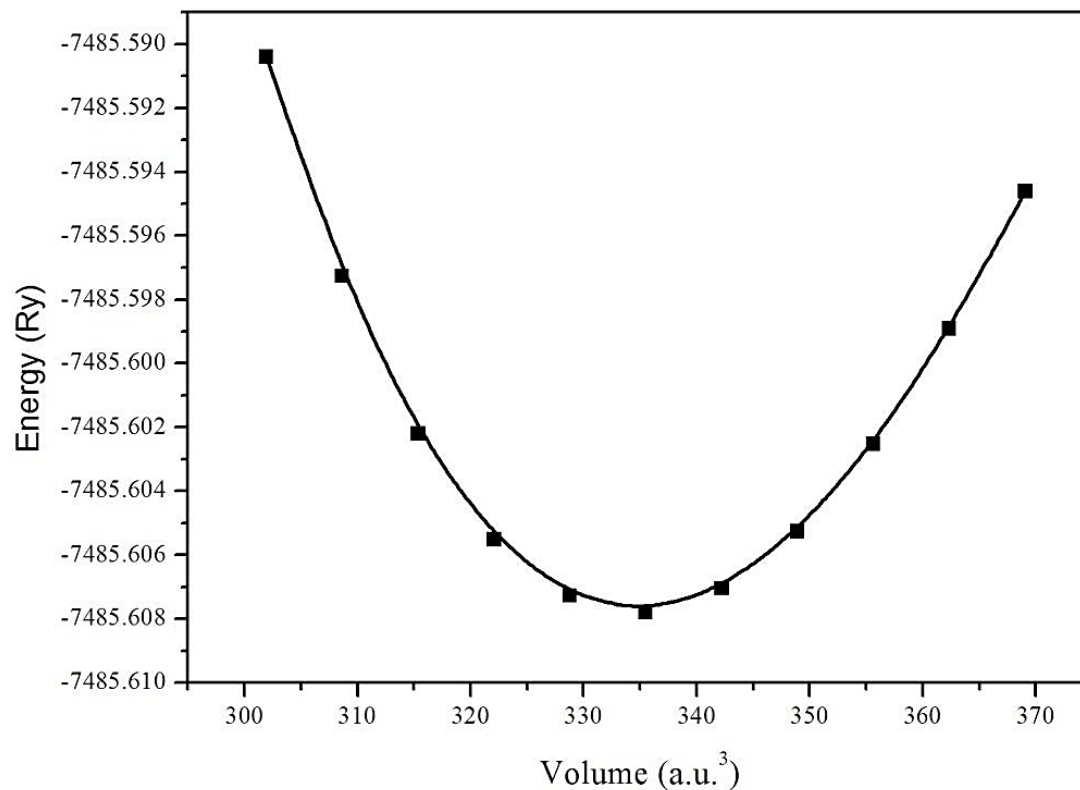


Figure 2. Volume optimization curve of ZnO material.

Table 1. Obtained lattice Parameter with various Approximations (exchange correlation function)

Approximation	Optimised Lattice Constant (Present Study)	Lattice constant (Previous Reported)
GGA-PBE	a=3.289Å, c=5.307Å	a=3.284 Å, c=5.296 Å [17] a=3.249 Å, c=5.206 Å [21] a=3.289 Å, c=5.308 Å [22]
GGA-PBESol		a=3.239 Å, c=5.227 Å [17]
GGA-PBE + U		a=3.254 Å, c=5.234 Å [17]

Electronic Properties

The calculated density of states (DOS) for ZnO material is similar for both spin up and spin down as shown in Figure 3. Zero energy shows Fermi energy level (E_F) while positive energy represents conduction band and negative energy as valence band. Total DOS is represented with black line while the red line and blue line show the density of states of Zn and O respectively. Total DOS shows semiconducting characteristics near E_F . An energy band gap of approximately 0.65 eV is observed at E_F which is the difference of energy between minimum of conductance band and maximum of valence band energy. Figure 4 represents the band structure of ZnO that is identical for both spin up and spin down. This band diagram indicates the energy band gap of 0.65 eV at the gamma line which also matches with the DOS. Observed energy band gap compared with the previously reported band gap is shown in Table 2. Value of band gap reported 0.83 eV by Ul Haq et al. using Perdew-Burke-Ernzerhof generalised gradient approximation (PBE-GGA) [23, 24] and 0.79 eV by Yaakob et al. using Local Density Approximation (LDA) [25]. The experimental energy band gap of ZnO material is 3.3 eV and 34. eV was reported by x-ray spectroscopy [26] and UV-spectroscopy [27], respectively. The variation in energy band gap is observed as the exchange correlation function treated in the simulation may relate the defects, surface and interface characteristics during the experimental fabrication process [28]. This energy band gap at room temperature gives the electron's excitation from valence to conduction band which lies in Infrared regions.

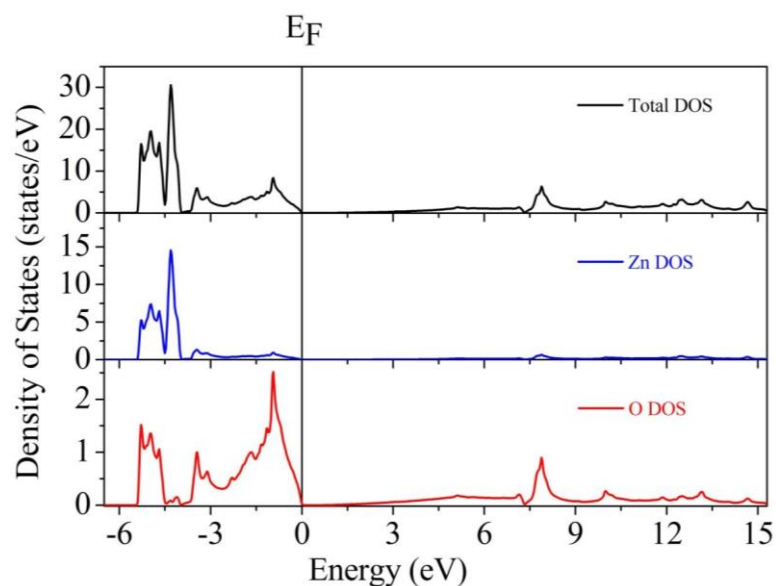


Figure 3. Density of States for ZnO material.

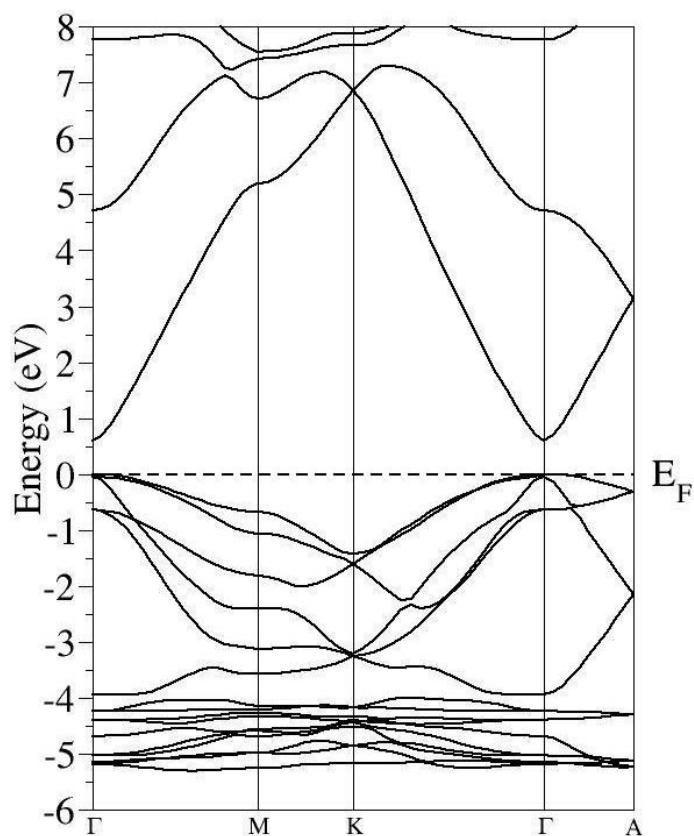


Figure 4. Band Structure of ZnO material.

Table 2. Obtained energy band gap with various approximation (exchange correlation function)

Approximation	Energy band gap (Present Study)	Energy band gap (Previous Reported)
GGA-PBE	0.65 eV	0.83 eV [24]
LDA		0.79 eV [25]
LDA + U		1.15 eV [25]
Experimental		3.3 eV [26], 3.4 eV [27]

Optical Properties

We have obtained the variation of optical parameters with respect to the incident energy in range between 0 to 13.6 eV such as real dielectric function (ϵ_1), imaginary dielectric function (ϵ_2), optical conductivity (σ), reflectivity (R), index of refraction (n), loss of energy (L), extinction coefficient (K) and coefficient of absorption (I) for ZnO material in the Figure 5. The dielectric function (ϵ) depends on frequency (ω) as equation 1 [29–31]:

$$\epsilon(\omega) = \epsilon_1(\omega) + i\epsilon_2(\omega) \quad (1)$$

Here ϵ_1 is real and ϵ_2 is imaginary dielectric functions that are vary with incident photon energy as shown in Figure 5(a) and 5(b) respectively. Peaks of interband absorption are observed in the whole spectral range. Value of ϵ_1 is 4.95 at zero energy and it reaches its maximum value of 5.59 at 0.80 eV that means the maximise degree of polarisation requires this energy. The peaks in the IR range (0 to 1.6 eV) indicate the presence of small energy band gaps in the band structure and DOS of the ZnO material. Interband absorption bands are initiate in the ultra-violet energy ranges. The next peak of ϵ_1 has been observed at 8.69 eV and after this energy its value decreases and becomes zero at 10.27 eV. This negative value of ϵ_1 is correlated to the limiting tunability of current to producing commercial application of ZnO material at higher energy [29].

The maximum value of ϵ_2 is 5.30 observed at 9.40 eV. It is correlated to dielectric losses of ZnO material. After this energy, material has been absorbing the energy and optical conductivity starts to decrease as shown in Figure 5(c). Small peak of σ is observed at 5.89 eV and the maximum value of σ is observed as 6635 per ohm per cm at 9.38 eV. After that, the energy value of σ fluctuates up and down that shows the instability at high energy and results in enhancement of reflectivity.

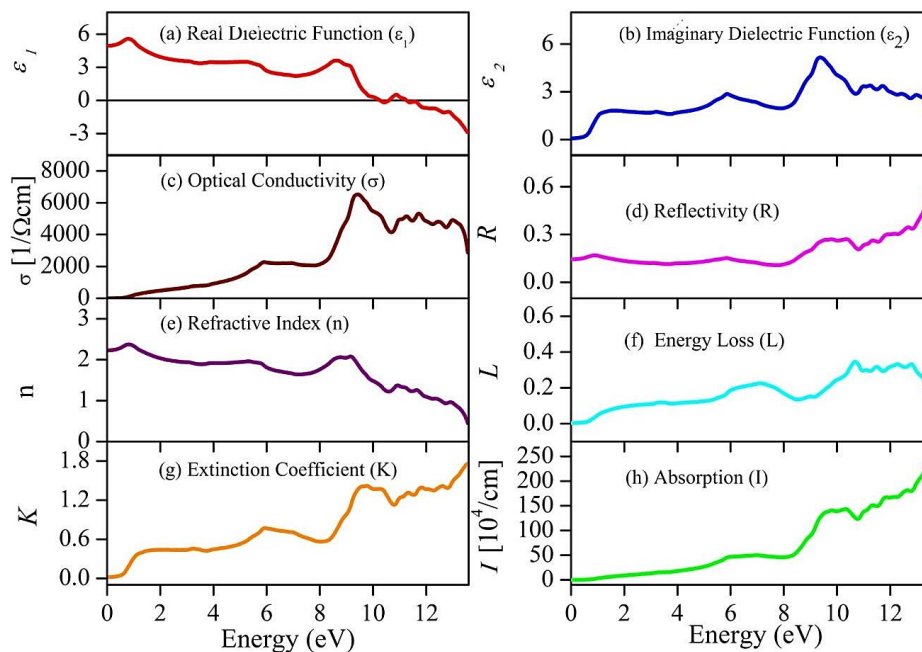


Figure 5. Optical parameters as a function of the energy of incident photons for ZnO material.

Refractive index (n) varies with energy as Figure 5(e) with 2.22 at zero energy. Maximum value of n was observed 2.42 at 0.80 eV similar to real dielectric constant ϵ_1 and decreases from 2.11 after the energy 9.10 eV. Energy loss of ZnO also increases with increasing the incident energy as shown in Figure 5(f). It observed that energy loss has maximum values where the conductivity has minimum at the energy points in the UV region i.e. 7.1 eV, 10.7 eV, 11.5 eV, 12.3 eV and 12.8 eV. Excitation coefficient (K) is a property that tells how strongly ZnO material absorbs or reflects electromagnetic radiation at a particular energy that is also represented in Figure 5(g). Its high value at high energy

tends to increase in the reflectivity (R) in Figure 5(d) as well as the absorption (I) in Figure 5(h). The reflectivity from the ZnO surface has observed 0.14 in a wide energy range from zero to 8.3 eV. The value of R starts to enhance and becomes more than 0.25 at incident energy of 9.1 eV and above energy. Transparency of ZnO will be high when reflectivity is less, this makes it a prominent material for display devices.

Variation of Optical conductivity in terms of per unit second of ZnO is also obtained and shown in Figure 6. The Initial value of σ is zero till 0.65 eV which also correlates the DOS in which we have observed the electronic transition band gap of 0.65 eV near to Fermi Energy. The value of σ increases on increasing incident energy. It shows that material is optically conductive in presence of visible light (nearly 1.63 to 3.26 eV) and ultraviolet light (nearly 3.2 to 100 eV). Major peaks of optical conductivity have been observed at 5.8 eV, 9.1 eV, 11.2 eV, 11.7 eV, 12.4 eV and 13.0 eV in the UV region. These optical characteristics of ZnO material show the high intensity of visible and UV radiations make it prominent for the manufacturing of optoelectronic devices such as LED, solar cell etc.

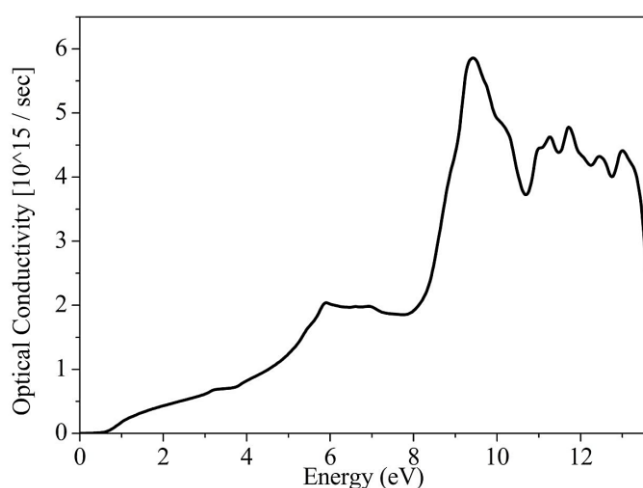


Figure 6. Optical conductivity per second as a function of the energy of incident photons for ZnO material.

CONCLUSION

Electronic, structure and optical properties of ZnO material computed with the help of density function theory in WIEN2k code. Structure of ZnO material stabilises in the Wurtzite form of hexagonal closed packed lattice. Observed value has 0.65 eV of direct energy band gap for ZnO which shows the semiconductor nature of materials with the help of DOS and band structure calculations. Optical parameters such as real dielectric function and imaginary dielectric function, index of refraction, optical conductivity, reflectivity, energy loss, absorption and extinction coefficient are discussed with variation of incident photon energy from 0-13.6 eV for the various applicability of the ZnO material. Optical conductivity of ZnO is conductive in presence of visible and ultraviolet light and prominent material and possible application in optoelectronic devices. Real dielectric function shows a wide range of energy to polarise the ZnO material. Reflectivity has observed less than 0.25 in the range of 0-10 eV that is good for display devices. Finally, we hope that this study helps researchers to make semiconductor devices such as MOSFET, TFT, LED, solar cell etc. with necessary amendments like doping and surface morphology that might tune the electronic, structural and optical properties as per need of the future generation.

Declaration of Competing Interest

We declare that we have not any known interests of competing financial assistance or personal relationships that could have emerged to domination the presented work in this manuscript.

Acknowledgement

The authors thank the DST-FIST, UGC-DSA, and RUSA agencies for supporting the computing services at the Physics Department of MLSU, Udaipur, Rajasthan.

REFERENCES

1. Kim, S., Kwon, H. J., Lee, S., Shim, H., Chun, Y., Choi, W., ... & Lee, S. Y. (2011). Low-power flexible organic light-emitting diode display device. *Advanced Materials*, 23(31), 3511–3516. <https://doi.org/10.1002/adma.201101066>
2. Rehman, A., Zeng, K., & Wang, Z. (2015, March). Display device-adapted video quality-of-experience assessment. In *Human vision and electronic imaging XX* (Vol. 9394, pp. 27–37). SPIE. <https://doi.org/10.1117/12.2077917>
3. Ma, L., & Shao, Y. F. (2020). A brief review of innovative strategies towards structure design of practical electronic display devices. *Journal of Central South University*, 27(6), 1624–1644. <https://doi.org/10.1007/s11771-020-4395-x>
4. Park, J., & Kim, S. (2022). Improving endurance and reliability by optimising the alternating voltage in Pt/ZnO/TiN RRAM. *Results in Physics*, 39, 105731. <https://doi.org/10.1016/j.rinp.2022.105731>
5. Isyaku, U. B., Khir, M. H. B. M., Nawi, I. M., Zakariya, M. A., & Zahoor, F. (2021). ZnO based resistive random access memory device: a prospective multifunctional next-generation memory. *IEEE Access*, 9, 105012-105047. <https://doi.org/10.1109/ACCESS.2021.3098061>
6. Lin, C. L., Tang, C. C., Wu, S. C., Juan, P. C., & Kang, T. K. (2015). Impact of oxygen composition of ZnO metal-oxide on unipolar resistive switching characteristics of Al/ZnO/Al resistive RAM (RRAM). *Microelectronic Engineering*, 136, 15–21. <https://doi.org/10.1016/j.mee.2015.03.027>
7. Franco, M. A., Conti, P. P., Andre, R. S., & Correa, D. S. (2022). A review on chemiresistive ZnO gas sensors. *Sensors and Actuators Reports*, 100100. <https://doi.org/10.1016/j.snb.2022.131674>
8. Lan, Y., Yang, G., Zhao, Y., Liu, Y., & Demir, A. (2022). Facet passivation process of high-power laser diodes by plasma cleaning and ZnO film. *Applied Surface Science*, 596, 153506. <https://doi.org/10.1016/j.apsusc.2022.153506>
9. Wang, Y., Zheng, Z., Wang, J., Liu, X., Ren, J., An, C., Zhang, S. & Hou, J. (2023). New Method for Preparing ZnO Layer for Efficient and Stable Organic Solar Cells. *Advanced Materials*, 35(5), 2208305. <https://doi.org/10.1002/adma.202208305>
10. Zeng, J., Qi, Y., Liu, Y., Chen, D., Ye, Z., & Jin, Y. (2022). ZnO-based electron-transporting layers for perovskite light-emitting diodes: Controlling the interfacial reactions. *The Journal of Physical Chemistry Letters*, 13(2), 694–703. <https://doi.org/10.1021/acs.jpcllett.1c04117>
11. Younis, A., Chu, D., & Li, S. (2013). Bi-stable resistive switching characteristics in Ti-doped ZnO thin films. *Nanoscale Research Letters*, 8, 1-6. <https://doi.org/10.1186/1556-276X-8-154>
12. Kim, D. H., Lee, D. W., Oh, J. Y., Won, J., Liu, Y., & Seo, D. S. (2022). Self-aligned liquid crystals and enhanced electro-optical properties on solution-processed aluminum gallium tin zinc oxide surfaces. *Journal of Materials Research and Technology*, 20, 291–302. <https://doi.org/10.1016/j.jmrt.2022.07.050>
13. Kawajiri, K., Tahara, K., & Uemiya, S. (2022). Life Cycle assessment of critical material substitution: Indium tin oxide and aluminum zinc oxide in transparent electrodes. *Resources, Environment and Sustainability*, 7, 100047. <https://doi.org/10.1016/j.resenv.2022.100047>
14. Wang, B., Zhang, Q., He, J., Huang, F., Li, C., & Wang, M. (2022). Co-catalyst-free large ZnO single crystal for high-efficiency piezocatalytic hydrogen evolution from pure water. *Journal of Energy Chemistry*, 65, 304–311. <https://doi.org/10.1016/j.jechem.2021.06.004>
15. Zhang, L. X., Zhao, M. M., Yin, Y. Y., Xing, Y., & Bie, L. J. (2022). Rich defects and nanograins boosted formaldehyde sensing performance of mesoporous polycrystalline ZnO nanosheets. *Rare Metals*, 41(7), 2292–2304. <https://doi.org/10.1007/s12598-021-01946-3>
16. Gupta, C.P., Sharma, S.K., Bhowmik, B., Sampath, K. T., Periasamy, C. & Sancheti, S., (2019) Development of Highly Sensitive and Selective Ethanol Sensors Based on RF Sputtered ZnO Nanoplates. *J. Electron. Mater.* 48, 3686–3691. <https://doi.org/10.1007/s11664-019-07127-4>

17. Harun, K., Yaakob, M. K., Taib, M. F. M., Sahraoui, B., Ahmad, Z. A., & Mohamad, A. A. (2017). Efficient diagnostics of the electronic and optical properties of defective ZnO nanoparticles synthesized using the sol–gel method: experimental and theoretical studies. *Materials Research Express*, 4(8), 085908. <https://iopscience.iop.org/article/10.1088/2053-1591/aa8151/meta>
18. Harun, K., Salleh, N. A., Deghfel, B., Yaakob, M. K., & Mohamad, A. A. (2020). DFT+ U calculations for electronic, structural, and optical properties of ZnO wurtzite structure: A review. *Results in Physics*, 16, 102829. <https://doi.org/10.1016/j.rinp.2019.102829>
19. Matur, U. C., Duru, I. P., & Akcan, D. (2022). Tracking optical properties of ZnO: Mg thin films: Experimental and first principles calculations. *Ceramics International*, 48(13), 19090-19097. <https://doi.org/10.1016/j.ceramint.2022.03.199>
20. Bashyal, K., Pyles, C. K., Afroosheh, S., Lamichhane, A., & Zayak, A. T. (2018). Empirical optimization of DFT+ U and HSE for the band structure of ZnO. *Journal of Physics: Condensed Matter*, 30(6), 065501. <https://iopscience.iop.org/article/10.1088/1361-648X/aaa441/meta>
21. Xia, C., Wang, F., & Hu, C. (2014). Theoretical and experimental studies on electronic structure and optical properties of Cu-doped ZnO. *Journal of alloys and compounds*, 589, 604–608. <https://doi.org/10.1016/j.jallcom.2013.11.066>
22. Yao, G. Y., Fan, G. H., Zhao, F., Ma, J. H., Chen, J., Zheng, S. W., Zeng, S.M., He, L.F. & Zhang, T. (2012). In assisted realization of p-type C-doped ZnO: A first-principles study. *Physica B: Condensed Matter*, 407(17), 3539–3542. <https://doi.org/10.1016/j.physb.2012.05.019>
23. Perdew, J. P., Burke, K., & Ernzerhof, M. (1996). Generalized gradient approximation made simple. *Physical review letters*, 77(18), 3865. <https://doi.org/10.1103/PhysRevLett.77.3865>
24. Ul Haq, B., Ahmed, R., Goumri-Said, S., Shaari, A., & Afaq, A. (2013). Electronic structure engineering of ZnO with the modified Becke–Johnson exchange versus the classical correlation potential approaches. *Phase Transitions*, 86(12), 1167–1177. <https://doi.org/10.1080/01411594.2012.755183>
25. Yaakob, M. K., Hussin, N. H., Taib, M. F. M., Kudin, T. I. T., Hassan, O. H., Ali, A. M. M., & Yahya, M. Z. A. (2014). First principles LDA+ U calculations for ZnO materials. *Integrated Ferroelectrics*, 155(1), 15–22. <https://doi.org/10.1080/10584587.2014.905086>
26. Dong, C. L., Persson, C., Vayssieres, L., Augustsson, A., Schmitt, T., Mattesini, M., Ahuja, R., Chang, C. L. & Guo, J. H. (2004). Electronic structure of nanostructured ZnO from x-ray absorption and emission spectroscopy and the local density approximation. *Physical Review B*, 70(19), 195325. <https://doi.org/10.1103/PhysRevB.70.195325>
27. Huang, M. H., Mao, S., Feick, H., Yan, H., Wu, Y., Kind, H., Weber, E., Russo, R. & Yang, P. (2001). Room-temperature ultraviolet nanowire nanolasers. *science*, 292(5523), 1897-1899. <https://doi.org/10.1126/science.1060367>
28. Clark, S. J., Robertson, J., Lany, S., & Zunger, A. (2010). Intrinsic defects in ZnO calculated by screened exchange and hybrid density functionals. *Physical Review B*, 81(11), 115311. <https://doi.org/10.1103/PhysRevB.81.115311>
29. Jain, V.K., Lakshmi, N., Jain, R. et al. Structural, Elastic, Electronic, Magnetic and Optical Properties of Spin Gapless Semiconducting Heusler Alloy Ti₂FeSb Using First-Principles Calculations. *J. Electron. Mater.* 50, 5857–5867 (2021). <https://doi.org/10.1007/s11664-021-09115-z>
30. Jain, V.K., Lakshmi, N., Jain, R. & Chandra, A. R. (2017), Electronic structure, magnetic and optical properties of quaternary Fe_{2-x}Co_xMnAl Heusler alloys. *J Mater Sci* 52, 6800–6811. <https://doi.org/10.1007/s10853-017-0918-8>
31. Jain, V.K., Lakshmi, N., Jain, R. & Chandra, A. R. (2019), Electronic Structure, Elastic, Magnetic, and Optical Properties of Fe₂MnZ (Z = Si, Ge, and Sn) Full Heusler Alloys: First-Principle Calculations. *J Supercond Nov Magn* 32, 739–749. <https://doi.org/10.1007/s10948-018-4751-3>